

# Very low frequency resistance fluctuations in thin films of $\text{La}_{0.67}\text{Ca}_{0.33}\text{MnO}_3$ with quenched disorder

Sudeshna Samanta\* and A. K. Raychaudhuri†

Department of Materials Science, S.N. Bose National Centre for Basic Sciences,  
Block JD, Sector III, Salt Lake, Kolkata 700 098, West Bengal, India

Joy Mitra‡

Department of Physics, Indian Institute of Science, Bangalore 560 012, India

(Received 29 January 2008; revised manuscript received 1 July 2008; published 25 July 2008)

In this paper we report the appearance of very low frequency ( $<1$  mHz) resistance fluctuations (noise) in strain relaxed rare-earth perovskite manganite films of  $\text{La}_{0.67}\text{Ca}_{0.33}\text{MnO}_3$  with quenched disorder grown on  $\text{SrTiO}_3$  (STO). The films show high degree of orientation and extremely low  $1/f$  noise. The observed spectral power clearly consists of two components: a Lorentzian part (arising from discrete fluctuators) that peaks near the ferromagnetic transition and a broadband  $1/f$  part that is essentially temperature independent. The noise power in the films with quenched disorder, interestingly, is orders of magnitude less than that seen in nearly strain free and uniformly strained thin films (thickness  $\leq 50$  nm) grown on  $\text{NdGaO}_3$  and STO, respectively. The discrete fluctuators seen in the films with quenched disorder are thermally activated with a high activation energy,  $\sim 0.7$  eV. Strain accommodation has been suggested as one of the likely mechanisms that leads to such a high thermal activation energy. The resistance fluctuation can be changed even by a small magnetic field ( $\leq 0.1$  T). The relative variance of the fluctuation has been observed to be proportional to the measured magnetoresistance ( $dR/dH$ ). We propose that the fluctuations arise from magnetization fluctuations, which couple to the resistance fluctuations by the magnetoresistance. The magnetization fluctuations arise from magnetic domains as well as from the fluctuating magnetization of the coexisting phases.

DOI: [10.1103/PhysRevB.78.014427](https://doi.org/10.1103/PhysRevB.78.014427)

PACS number(s): 75.47.Lx, 72.70.+m, 75.70.-i, 71.30.+h

## I. INTRODUCTION

The mixed-valence manganites  $\text{Ln}_{1-x}\text{D}_x\text{MnO}_3$  (where Ln is a rare earth and D is a divalent alkaline-earth atoms) are interesting<sup>1,2</sup> because of the interplay between charge, spin, orbital, and structural degrees of freedom. This gives rise to a multitude of ordered phases and thus a very rich phase diagram. There are varieties of ordered ground states for manganites, ranging from ferromagnetic metallic state to charge and orbital ordered insulating states that can also have antiferromagnetic spin order. The presence of interactions of comparable strengths provide a delicate energy balance so that ground states sometimes may not be homogeneous, leading to mesoscopic electronic phase separation.<sup>3,4</sup> The electronic phase separation that leads to this inhomogeneity couples to a number of physical properties. For the specific system  $\text{La}_{1-x}\text{Ca}_x\text{MnO}_3$  for  $x=0.22-0.4$  (optimal  $x=0.33$ ), there is a well defined paramagnetic to ferromagnetic transition at  $T_C$  on cooling and also a transition from a polaronic insulating state at high temperature to a ferromagnetic metallic state at low temperature, which results in a peak in resistivity at  $T_p$ . Typically in good manganite samples,  $T_C \approx T_p$ .

In addition to conventional transport measurements, noise has been investigated on  $\text{La}_{0.67}\text{Ca}_{0.33}\text{MnO}_3$  (LCMO) films (of varying quality<sup>5,6</sup>) and even on single crystals.<sup>7,8</sup> Noise spectroscopy has been used earlier to study the dynamics of phase separation.<sup>9-12</sup> While most of the studies investigated the noise with spectral power  $S_v(f) \sim 1/f$  (the  $1/f$  noise), a wealth of physical information came from discrete fluctuators that typically occur in small temperature windows for

$T < T_C$ . These fluctuators have been seen in single crystal and also in uniformly strained (or low strain) epitaxial films, and they contribute a Lorentzian-type term to the noise spectral power  $S_v(f)$ . These fluctuators that were observed close to the transition temperatures  $T/T_C \approx 0.90-0.95$  have a volume scale in the range of  $10^4-10^5$  unit cells<sup>13</sup> although the exact nature of their origin may not be clearly established. [Note that by discrete fluctuators, we imply fluctuators that give rise to random-telegraphic noise (RTN).<sup>14</sup>] The resistance fluctuation in these films is generally attributed to electronic phase separation and phase coexistence of the high resistance (paramagnetic) and low resistance (ferromagnetic) phases. It is the coexistence of these phases and the dynamical nature of the phase equilibrium that determines the time scale of the resistance fluctuations. We note that coexisting phases giving rise to discrete fluctuators have been seen in the case of charge ordering transition. Existence of low frequency discrete fluctuators showing RTN (along with broadband  $1/f$  noise) have been also seen in single crystals of  $\text{Pr}_{0.7}\text{Ca}_{0.3}\text{MnO}_3$ , which shows a transition from a paramagnetic insulating state to a charge ordered insulating state.<sup>9</sup> The discrete fluctuators seen at this transition are thermally activated with a rather long relaxation time and high activation energy  $E_a \approx 0.45$  eV. The activation energy of the discrete fluctuators reported so far in  $\text{La}_{1-x}\text{Ca}_x\text{MnO}_3$  ( $x \sim 0.30-0.33$ ), however, have a much lower value of  $E_a$ . The observed activation energy is typically much less than 0.1 eV. One interesting question that arises is whether one can clearly observe discrete fluctuators with large activation energy near the  $T_C$  of LCMO. Discrete fluctuators with large  $E_a$  are expected to have long relaxation time and thus contribute

to the power spectra at very low frequency only. The challenge of observing such a low frequency noise from discrete fluctuators is to reduce the  $1/f$  noise that can become substantial in this frequency region. We show in this paper that a very low  $1/f$  noise can be achieved in oriented films of  $\text{La}_{0.67}\text{Ca}_{0.33}\text{MnO}_3$ , which have quenched disorder created by strain relaxation. Interestingly, the  $1/f$  noise in these films can even be less than that seen in low strain LCMO films grown on  $\text{NdGaO}_3$  (NGO). Such a low  $1/f$  noise in the strain relaxed films facilitates observation of very low frequency discrete fluctuators.

The role of strain and the microstructure are very important in films of manganites. Depending on the lattice mismatch with the substrate and the thickness of the film, the LCMO films with thickness  $\leq 50$  nm can have very low strain (grown on NGO) or uniformly strained [grown on  $\text{SrTiO}_3$  (STO)], and they show a clean terrace and step-type growth pattern. Thicker films of  $\text{La}_{0.67}\text{Ca}_{0.33}\text{MnO}_3$  (grown on oriented STO substrate) are strain relaxed and the microstructure shows platelet structure (columnar type) with misfit dislocations threading the platelet boundaries.<sup>15</sup> These are the films with quenched disorder. There has been lack of a systematic investigation of low frequency resistance fluctuation in these types of films. In the present investigation, we have focused mainly on such well characterized strain relaxed films with a specific type of quenched disorder. We show that these films can show very low  $1/f$  noise down to very low frequency ( $f \geq 10$  mHz) and in the frequency range below that, discrete fluctuators with large thermal activation energy show up. The noise spectroscopy experiment was carried out in the very low frequency ( $0.25 \text{ mHz} \leq f \leq 1 \text{ Hz}$ ) range and in the temperature range of 100–300 K with specific focus in the region close to the ferromagnetic transition temperature.

## II. EXPERIMENT

The LCMO films were grown on single crystalline substrates by pulsed laser deposition (PLD) following the standard procedure.<sup>16</sup> Some of the relatively thicker films were also prepared by the chemical solution deposition (CSD) technique.<sup>17</sup> The CSD synthesized films grown on single crystalline substrates have characteristics that are very similar to the same films grown by the PLD technique. The detailed investigation on the discrete fluctuators showing RTN in the time series were carried out on films (thickness of 500 nm) grown on STO. We have also carried out measurements on LCMO films (thickness of 50 nm) grown on NGO, which have very little strain, and on uniformly strained film of LCMO with thickness of 50 nm grown on STO.

### A. Physical characterization

The films grown have been characterized by x-ray diffraction (XRD), scanning electron microscope (SEM), and scanning probe techniques such as atomic force microscopy (AFM) and scanning tunneling microscope (STM). The  $(\theta - 2\theta)$  XRD profile confirms that the films grown maintain their orientation with the substrate. Representative data on

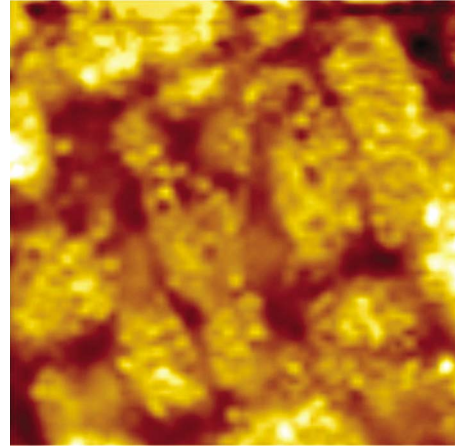


FIG. 1. (Color online) Topography ( $t$ ) on LCMO/STO (200 nm) film at 265 K,  $t:[(\Delta x \mu\text{m} \times \Delta y \mu\text{m} \times \Delta z \text{nm})](0.16 \mu\text{m} \times 0.16 \mu\text{m} \times 0.6 \text{nm})$ .

such films are given in Refs. 15 and 16. The 50 nm film grown on STO and NGO shows step and terrace growth patterns, as expected from uniformly strained films or strained films with very little strain. The STM and AFM images of the films are similar to the images of similar films that we reported before<sup>16</sup> and are not shown here to avoid duplication. The strain relaxed thicker films show platelets. For example, in Fig. 1, we show the STM (topographic image) of the 200 nm strain relaxed film. The platelets have an average size of  $\sim 40$ – $50$  nm, as shown in Fig. 1. For the 500 nm film, the platelet structure is qualitatively similar but they have larger size,  $\sim 100$  nm. The platelets so formed have coherent boundaries and have columnar structure. These are different from grain boundaries as seen in polycrystalline films, which form between crystallographic grains with random orientation. A cross-sectional transmission electron microscopy (XTEM) image on similar 200 nm films<sup>15</sup> shows that the growth is columnar and platelet boundaries have misfit dislocations that span from the substrate to the film surface with the average spacing between these misfit dislocations matching the platelet sizes. Thus the quenched disorder in these films consists of mainly the misfit dislocations that form during the strain relaxation to accommodate the strain due to lattice mismatch. Thus the strain relaxed films on which we have carried out the main investigation are different from the thinner uniformly strained films grown on STO and NGO. This difference, as we will see below, is reflected in the low frequency resistance fluctuations.

The STM was also used to map the local tunneling conductance  $g$  at a fixed bias and thus map the local inhomogeneity. The mapping, which we call the local conductance map (LCMAP), has been described elsewhere.<sup>18</sup> This technique allows mapping of the local density of state at the Fermi level  $[N(E_F)]$ . Since  $N(E_F)$  is expected to show spatial fluctuations as one scans the phase-separated regions, one can map the extent of spatial phase separation.

The resistivity ( $\rho$ ) was measured down to 20 K by a four-probe ac biasing technique.  $\rho$  shows a distinct peak corresponding to the transition from the high-temperature insulating polaronic phase to the low-temperature metallic phase. In

TABLE I. Electrical characterizations of samples used

Sample	Thickness (nm)	$\rho_{\text{peak}}$ (mOhm-cm)	$\rho_{20 \text{ K}}$ (mOhm-cm)	$T_p$ (T)
LCMO/STO	50	130	0.3	215
LCMO/NGO	50	20	0.2	268
LCMO/STO	500	45	1	270

the film grown on NGO, the strain being least,  $\rho_{\text{peak}} \approx 20$  mOhm cm at  $T_p \approx 268$  K and residual  $\rho \approx 0.2$  mOhm cm. In the uniformly strained 50 nm film grown on STO, the  $T_p$  is severely suppressed ( $\sim 215$  K) and the  $\rho_{\text{peak}}$  is considerably larger at about 130 mOhm cm. This film, however, has a low residual  $\rho \approx 0.3$  mOhm cm. In the strain relaxed films, typical peak in  $\rho$  occurs at temperature  $T_p \approx 270$  K, which is similar to the unstrained films or single crystals. The film shows a peak in  $d\rho/dT$  at a temperature  $\sim 228$  K. The films have a typical  $\rho_{\text{peak}} \approx 45$  mOhm cm and a residual resistivity of  $\sim 1$  mOhm cm. The strain relaxation brings down the  $\rho_{\text{peak}}$  compared to uniformly strained films (like those grown on STO) but the presence of the platelet boundaries increase the residual resistivity. All relevant transport data have been collected in Table I.

The films have also been characterized using magnetization measurement [ $M(T)$  vs  $T$  and  $M-H$ ] using a vibrating sample magnetometer (VSM). The 500-nm-thick strain relaxed film on which we did most of the noise measurements undergoes a ferromagnetic transition at  $T_C = 266$  K. The magnetization reaches technical saturation for  $H \leq 0.15$  T. The typical films have a saturation moment in the range of  $6 \times 10^{-3}$  emu. The coercive field  $H_C$  is typically  $\leq 0.01$  T.

### B. Noise measurement

The resistance fluctuation (noise) measurements were carried out using digital signal processing (DSP) based ac technique, which allows simultaneous measurement of background noise as well as bias dependent noise from the sample.<sup>19,20</sup> The technique has been used by us in the past to study resistance fluctuations in a number of systems, including the charge ordered manganites.<sup>9</sup> The apparatus was calibrated down to a spectral power  $S_V(f) = 10^{-20}$  V<sup>2</sup>/Hz by measuring the Nyquist noise ( $S_V = 4K_B TR$ ) for a calibrated resistor at a known temperature. A complete set of time series data at each temperature consists of  $5 \times 10^6$  data points or more and from which the spectral power density  $S_V(f)$  was determined numerically by using fast Fourier transform (FFT).

For long time data-acquisition process, which is needed here, we have to subtract a monotonous long time drift by a least-square fit to the data. We have ensured that such a subtraction does not distort the power spectrum. The low frequency limit of the spectral power has been limited by the drift process and the temperature control was sufficiently good to ensure stability of such low frequency (long time series) data. We found that the typical temperature drift for a set of time series data is  $\approx 2$  mK (time taken is  $\sim 2$  h). The lowest frequency limit ( $f_{\text{min}}$ ) has been imposed by the tem-

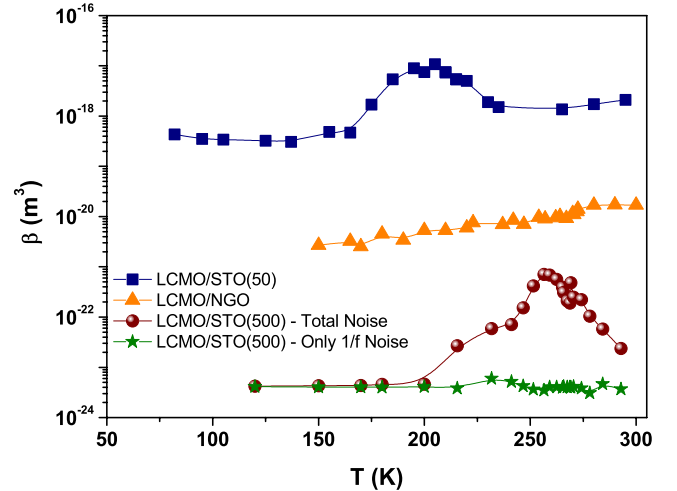


FIG. 2. (Color online) Temperature variation of  $\beta$  for LCMO/STO (50 nm), LCMO/NGO, and LCMO/STO (500 nm) film.

perature stability. The relative variance of the resistance fluctuation  $\langle (\Delta R)^2 \rangle / R^2$  within the detection bandwidth ( $f_{\text{min}} \rightarrow f_{\text{max}}$ ) was obtained by integrating the power spectrum  $\equiv (1/V^2) \int_{f_{\text{min}}}^{f_{\text{max}}} S_V(f) df$ . For comparison of data between different films, we used the quantity  $\beta = \Omega \frac{\langle (\Delta R)^2 \rangle}{R^2}$ , where  $\Omega$  is the volume of the region of the film on which the noise measurement has been made.

## III. RESULTS OF NOISE MEASUREMENT

### A. 1/f Noise

The power spectra of unstrained film (thickness of 50 nm) grown on NGO and those of uniformly strained films grown on STO show only  $1/f$  dependence. However, the spectral power in the uniformly strained film grown on STO is much larger (by nearly two orders of magnitude), as can be seen in Fig. 2 where the quantity  $\beta$  has been plotted as function of temperature for the films. The noise peaks close to  $T_C$  in the film grown on STO. However,  $\beta$  in the film grown on NGO does not show any peak and shows a small decrease as it is cooled through  $T_p$ . In the film grown on STO, the  $1/f$  noise is too large for observation of any discrete fluctuators. However, the existence of the discrete fluctuators (close to  $T_p$ ) cannot be ruled out. A clean separation of the noise power between a  $1/f$  dependence and the Lorentzian-type contribution from discrete fluctuators was not possible. The data presented here match very well with those reported before on STO and NGO films.<sup>21</sup>

For the films with quenched disorder, the observed noise is very different. In particular, in the film with thickness of 500 nm, one can clearly separate out the  $1/f$  part and the contribution from the discrete fluctuators. As can be seen from Fig. 2, this film has a  $\beta$  that is less than that seen even in the LCMO (50 nm) grown on NGO. The total noise has a  $1/f$  noise component that is essentially temperature independent. At  $T = 300$  K (where the noise has substantial  $1/f$  contribution), the Hooge parameter<sup>22</sup> has a value of  $\sim 500$ . This film, close to the transition region, also shows very low fre-



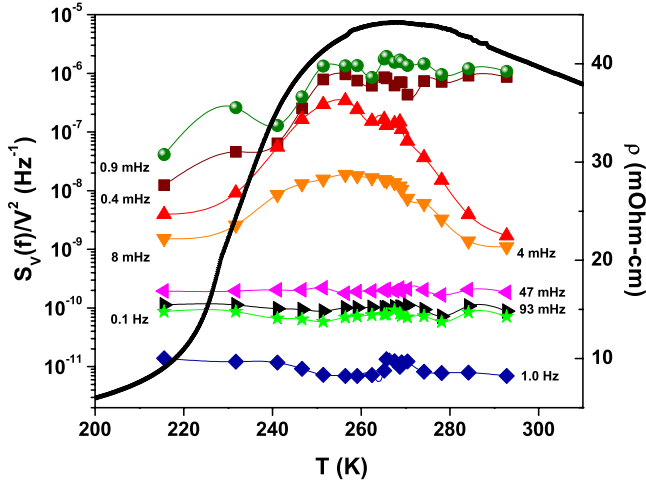


FIG. 3. (Color online) The scaled spectral power  $S_V(f)/V^2$  measured at few representative frequencies as a function of  $T$  along with the sample resistivity  $\rho(T)$ .

quency noise. We will discuss this in the next subsection. This type of noise behavior was repeatedly seen in these films, which have the type of quenched disorder that is created by strain relaxation. Thus not only strain but also microstructure can change the nature of resistance fluctuation in these films, not only quantitatively (by orders of magnitude) but also qualitatively.

**B. Lorentzian-type fluctuation in strain relaxed films**

In Fig. 3, we show the spectral power  $S_V(f)/V^2$  for the low noise 500 nm film measured at few representative frequencies as a function of  $T$  along with the sample resistivity  $\rho(T)$ . We find that at low frequencies ( $\leq 10$  mHz), spectral power has a nontrivial temperature dependence around the transition temperature while at higher frequencies ( $\geq 10$  mHz), there is no dependence on temperature. We elaborate on this spectral dependence later on.

In Fig. 4 we plot the spectral power as a function of frequency at few representative temperatures, which encompass the transition region. The data are plotted as  $fS_V(f)/V^2$  to show the clear deviation of the spectral power from the

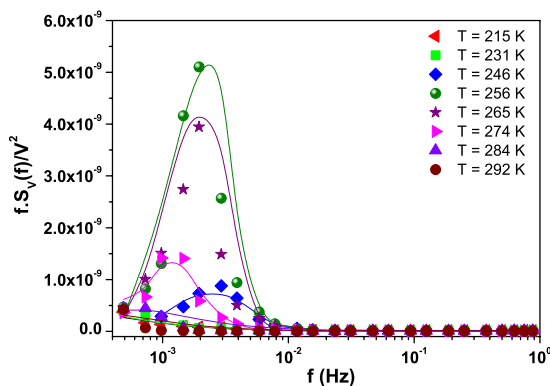


FIG. 4. (Color online) The spectral power  $fS_V(f)/V^2$  measured at few representative temperatures as a function of  $f$ .

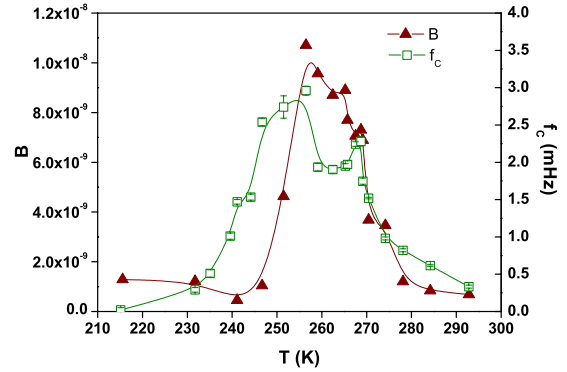


FIG. 5. (Color online) The temperature dependence of  $B(T)$  and Lorentzian corner frequency  $f_c(T)$ .

$1/f$  dependence. For  $f \geq 10$  mHz, the spectral power exhibits a clean  $1/f$  dependence (which remains mainly temperature independent). At lower frequency  $S_V(f)$  has strong deviation from  $1/f$  dependence. The deviation is most prominent around the transition region. We have fitted the spectral power at each temperature  $T$  in the complete frequency region by the following relation [using Eq. (1)], which consists of a  $1/f$  term and a Lorentzian with a temperature-dependent corner frequency  $f_c(T)$ ,

$$\frac{S_V(f)}{V^2} = \frac{A(T)}{f} + \frac{B(T)f_c(T)}{f^2 + f_c(T)^2}. \tag{1}$$

The fit is shown in Fig. 4 and, as can be seen, the two parts are well separated in the frequency domain. The Lorentzian-type spectral power can be observed for  $f \leq 0.01$  Hz. The temperature-dependent constants  $A(T)$  and  $B(T)$  are obtained from the fitted data and they give relative weights of the two contributions. Plots of  $f_c(T)$  and  $B(T)$  as functions of  $T$  are shown in Fig. 5. While  $A(T)$ , the weight of the  $1/f$  term has very little temperature dependence; both  $f_c(T)$  and  $B(T)$  show nontrivial temperature dependence, in particular, around the transition region ( $T/T_C \approx 0.9-1.0$ ) where they become substantially large. Both of them reach a maximum at  $T/T_C = 0.95$ . The observed corner frequencies  $f_c(T)$  are low and  $< 5$  mHz. (Note that in earlier studies, the reported spectral range was for  $f > 100$  mHz. As a result these fluctuations could not be observed.) The data presented here is for a typical film. We found that this behavior is reproducible in a number of similar films studied by us. We note that discrete fluctuators in this temperature range were seen in epitaxial films grown on NGO.<sup>21</sup> We are not aware of any investigation that has investigated this type of fluctuations in a strain relaxed film with quenched disorder.

The Lorentzian-type contribution to the power spectrum (with a corner frequency  $f_c$ ) arises from the discrete fluctuators, which show RTN in the time series. As an example, we show the time series in Fig. 6 at 250 K where the Lorentzian-type power spectrum peaks up. This time series shown in Fig. 6 is a typical example. The RTN-type time series shows that the fluctuators causing the resistance fluctuations are of two-level type. However, it appears that there may be two superimposed two-level fluctuators with different levels. The

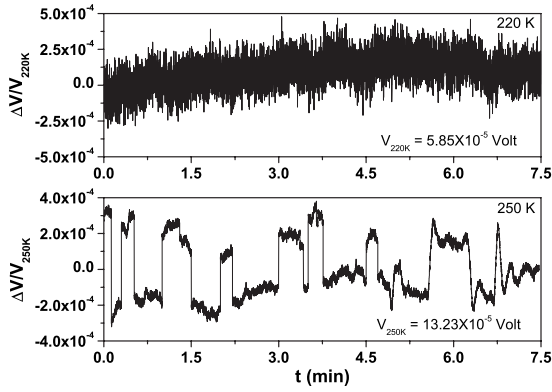


FIG. 6. The time series data at two representative temperatures.  $V_{220\text{ K}}$  and  $V_{250\text{ K}}$  are the sample bias voltages at 220 and 250 K, respectively.

time periods associated with them are similar. The average time scale for the two-level-fluctuators (TLF)  $\tau_C$  is related to the corner frequency  $f_C$  seen in the power spectrum by the relation  $\tau_C^{-1} = 2\pi f_C$ . The data show that, near the ferromagnetic transition, the TLF fluctuators become measurable in the time scale of the measurements ( $f_C$  becomes more than 0.25 mHz) and also their number density increases.

### C. Effect of magnetic field on resistance fluctuation in strain relaxed films

The resistance fluctuation has a distinct dependence on the applied magnetic field ( $H$ ), particularly at low fields. In Fig. 7, we plot relative resistance fluctuations  $\beta$  with  $H$  at few representative temperatures. In the top part of the same graph, we show a part of the  $M$ - $H$  curve at  $T=250\text{ K}$  where the noise power shows a peak. The  $M$ - $H$  curve establishes the scale of the magnetic field. The field dependence becomes very weak as  $T \rightarrow T_C$ . Power spectrum (not shown to avoid repetition) shows that most of the spectral weight comes from the region with  $f \leq 10\text{ mHz}$ . The noise is suppressed initially for low magnetic field ( $\leq 0.05\text{ T}$ ), which is similar to (but somewhat lower than) the value  $H_C$  of the film. Beyond that it starts rising for higher fields and shows saturation. The saturation magnetic field is lower than the technical saturation seen in  $M$ - $H$  curve. It is important to note that such a small field has substantial effect on the noise power. One important observation merits attention although the magnitude of the resistance fluctuation has strong dependence on the magnetic field: the value of the corner frequency  $f_C$  has negligible dependence on the magnetic field. This is in contrast to past studies.<sup>7</sup>

## IV. DISCUSSION

Our observation shows that the strain (as well as the microstructure) plays an important role in determining the magnitude of noise power as well as the spectral nature of the resistance fluctuation in manganite films. In particular, in films with quenched disorder, there is a significant drop in the noise and it is even lower than that of the film grown on the NGO, which has very little strain. This is a particularly

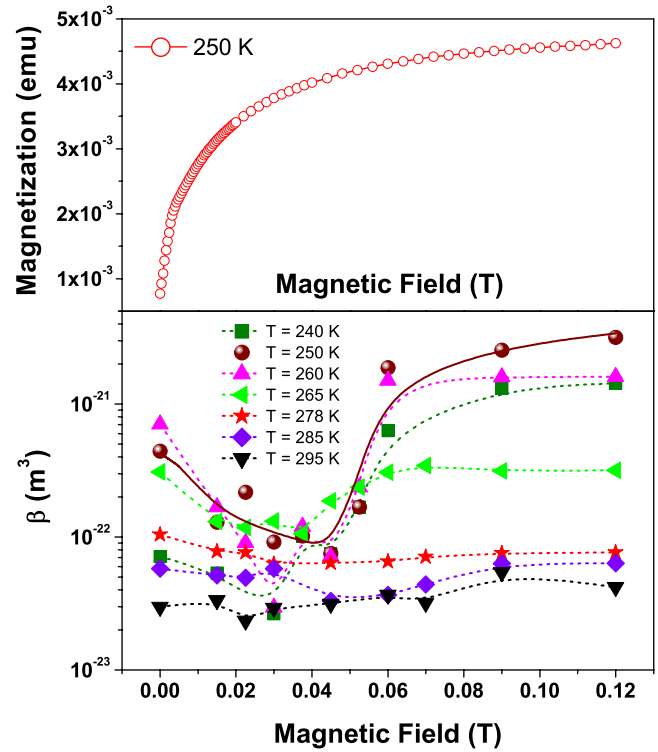


FIG. 7. (Color online)  $\beta$  as function of magnetic field  $H$  at few representative temperatures. The upper panel shows the saturation of the magnetization at 250 K.

important observation that quenched disorder can lead to suppression of noise. One way that we may justify this observation is if the fluctuators that contribute to the noise in the films with quenched disorder have very large energy for thermal activation. In that case only a small number of fluctuators will be observable in the frequency window of the resistance noise measurements and it is the slow kinetics that makes most of the fluctuators unobservable in the observation window. Large energy for thermal activation ( $E_a$ ) can arise if the fluctuation process involves long-range strain accommodation that would be needed to have coexisting phases. Although there is no direct experimental evidence, there are suggestions that coexisting phases can have martensite-type long-range strain accommodation.<sup>23</sup> In case of the LCMO with  $x \approx 0.3-0.35$ , the coexisting phases close to  $T_C$  are the ferromagnetic metallic (FMM) phase and the polaronic paramagnetic insulating state. There is a difference in the Jahn-Teller distortion around the  $\text{Mn}^{3+}$  ions in the two phases, and when phases are coexisting in dynamic equilibrium, there will be small strain accommodation. The physical size of such strain accommodation will be limited by the misfit dislocations. In that case the strain accommodation occurs over regions with diameter of approximately 50–100 nm and thickness limited by the film thickness (500 nm). With a bulk modulus of  $B=190\text{ GPa}$ , as reported for LCMO, the strain accommodation will lead to  $E_a \approx 0.25-1.0\text{ eV}$  even for a small strain of only  $\epsilon \sim 2 \times 10^{-5}$ .

The corner frequency  $f_C$  is small and has a strong dependence on temperature close to  $T_C$ . At lower temperatures (for  $T < 250\text{ K}$ ) when  $f_C$  increases in heating, one can associate a

thermally activated process for relaxation of the two-level fluctuators. Using the limited range of data available ( $T < 250$  K) and the Arrhenius relation  $f_C = f_0 \exp(-E_a/k_B T)$ , we evaluated the attempt frequency,  $f_0 \approx 4.5 \times 10^{14}$  Hz, and the activation energy,  $E_a \approx 0.7$  e.V. The high value of the activation energy justifies the very low value of  $f_C$  seen in these materials. This observation of high  $E_a$  supports the suggestion made in the previous paragraph. We note that fluctuators with such high  $E_a$  have been seen near the charge ordering transition before.<sup>9</sup> We also note that there is a decrease in  $f_C$  for  $T > 250$  K. We do not have any clear explanation for this behavior. This can occur due to a hardening of  $E_a$  and/or a decrease in the attempt frequency. It may also be that the RTN that contributes to the spectral power in this region may have a complex temperature-dependent behavior. As pointed out before, the RTN observed may actually be a superposition of two RTN processes with their corner frequencies having different temperature dependences. The nontrivial temperature dependence of  $f_C$  may indeed be a reflection of this.

The magnitude of the Lorentzian-type noise that arises from the discrete fluctuators can be tuned even by a small field. However, it is important to note that the magnetic field does not change the corner frequency  $f_C$ . This is unlike the previously observed reports where the time scale can be tuned by the applied field.<sup>7</sup> In our case, the absence of an effect on  $f_C$  is expected because the applied field is small and the scale of  $MH$  is far too small compared to the activation energy  $E_a$ . As an origin for the dependence of the resistance noise on the magnetic field, we note that the local resistance can change if they are coupled to the magnetization  $M$ . The only quantity that changes substantially at temperatures close to  $T_P$  and that can also be changed by such a low field is the magnetization  $M$ . The resistance fluctuation at very low frequency that appears can be related to the fluctuation in local magnetization. Such a fluctuation will couple to the resistance fluctuation via magnetoresistance (MR) ( $dR/dH$ ) and the derivative of the magnetization  $dM/dH$ . The low-field magnetoresistance at different  $T$  are shown in Fig. 8. The  $dR/dH$  has been obtained by actual measurements in low field ( $H \leq 0.1$  T). The  $R$  decreases linearly in  $H$  and  $dR/dH$  peaks near  $T_C$ , as shown in the inset of Fig. 8. The magnetization fluctuation  $\langle(\Delta M)^2\rangle$  will give rise to the resistance fluctuation:

$$\frac{\langle(\Delta R)^2\rangle}{R^2} = \xi \left( \frac{1}{R} \frac{dR}{dM} \right)^2 \langle(\Delta M)^2\rangle, \quad (2)$$

where  $\xi$  is the constant that takes care of the fact that the current flow is inhomogeneous and, if the fluctuators sit on a path of high current concentration, even a small magnetization fluctuation leads to much larger resistance fluctuations. Such an effect has been also seen in past studies on discrete fluctuators.<sup>13</sup> Since  $dR/dM = \frac{dR/dH}{dM/dH}$  one would expect  $\frac{\langle(\Delta R)^2\rangle}{R^2} \propto dR/dH$ . Such a linear relation exists, as can be seen in Fig. 9. Very close to and above  $T_C$ , the linearity breaks down because the magnetization itself collapses.

The fluctuation in magnetization ( $\Delta M$ ) can occur due to two reasons. First, close to  $T_C$ , a contribution due to domain

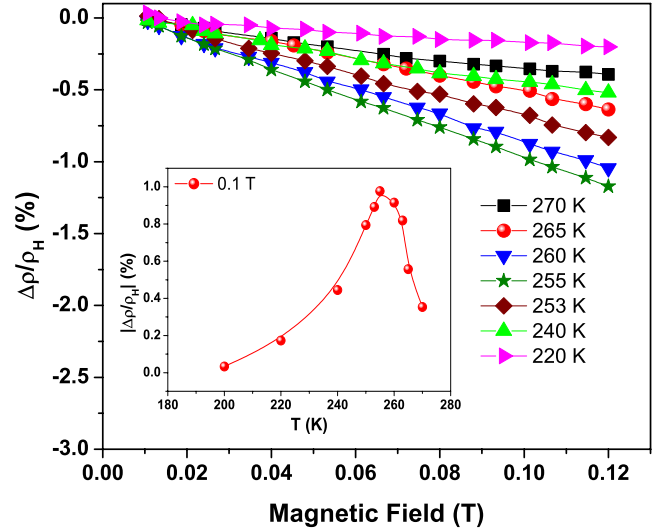


FIG. 8. (Color online) MR as a function of magnetic field for few representative temperatures. MR as a function of temperature (measured with field 0.1 T) is shown as an inset.

rotation can arise. The contribution of the domain rotation to  $\frac{\langle(\Delta R)^2\rangle}{R^2}$  is expected to decrease as  $H$  increases and eventually at  $H \geq H_C$ , this contribution should subside. Thus a variation  $\frac{\langle(\Delta R)^2\rangle}{R^2} \propto 1/H^\alpha$  is expected. Another contribution to  $\Delta M$  can arise from the coexisting phases. The two coexisting phases that give rise to the noise have different magnetization. One of the phases with lower resistance will be the ferromagnetic phase with higher magnetization, and the other higher resistance phase will be paramagnetic or even antiferromagnetic and will have low moment. The contribution to  $\Delta M$  due to difference in the magnetization of the two coexisting phases is thus expected to become larger as  $M$  becomes larger on application of the field. A simple expectation will be  $\frac{\langle(\Delta R)^2\rangle}{R^2} \propto M^n$ , where  $n \approx 2$ . In the range of our data ( $H$  below technical saturation),  $M \propto H^\eta$ , where the observed  $\eta \approx 0.25-0.27$ . Thus one would expect  $\frac{\langle(\Delta R)^2\rangle}{R^2} \propto H^\gamma$ , where  $\gamma \approx n\eta$ . We fitted the experimental field dependence of the resistance fluctuation to the empirical relation  $\frac{\langle(\Delta R)^2\rangle}{R^2} = A/H^\alpha + B(H-H_C)^\gamma$  and find that such a relation indeed fits the data,

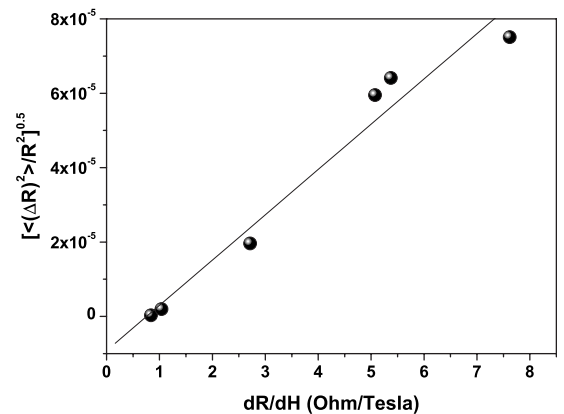


FIG. 9.  $\sqrt{\frac{\langle(\Delta R)^2\rangle}{R^2}}$  as a function of  $dR/dH$  at temperatures  $T < T_C$ .

as shown by the solid line in Fig. 7. The observed  $\gamma \approx 0.4$  compares well with expected estimate of  $\approx 0.5$ . The above discussion strongly suggests that the observed resistance fluctuation arises from the magnetization fluctuation and the coupling occurs by magnetoresistance.

At the end we would like to discuss, although not conclusively, whether one can establish any direct connection between the temporal fluctuation, as recorded by the noise spectral power, and the spatial fluctuation that may be probed by such local probes like STM. The variation of local fluctuation in  $g$ , as measured by STM, shows that these films have substantial degree of spatial phase separation. However, as the discussion will show below, the establishment of such a correlation between these fluctuations, although tempting, has its problems, which is related to the time scales of the image acquisition in the local probe methods and thermal drift in the subsequent scans. The coexisting phases are electronically distinct and thus are expected to have different density of state at the Fermi level  $[N(E_F)]$ . Thus  $N(E_F)$  is expected to show spatial fluctuations as one scans the local tunneling conductance  $g$  [ $g \propto N(E_F)$ ] of the phase-separated regions by the STM. From the measured local map of  $g$ , we computed the root-mean-square relative fluctuation in the local tunneling conductance  $\langle \Delta g^2 \rangle^{0.5} / g$ . The temperature variation of the  $\langle \Delta g^2 \rangle^{0.5} / g$  for the three classes of the films is shown in Fig. 10. The spatial fluctuation in the films peak around  $T/T_p \approx 1-0.95$ . It is largest in the uniformly strained 50 nm film grown on STO, which reaches a peak close to  $T_p$  that can be as large as one. The map of  $g$  from which the spatial fluctuation has been computed has been taken over a time scale of  $\sim 1$  s. It can be regarded as a “snapshot.” This is faster than the time scale over which the RTN occurs. In fact if we keep the STM tip at a point on the sample, we can clearly observe the RTN-type fluctuation in the time series of the tunneling current. This is in addition to the usual  $1/f$  noise of the STM amplifier. If the data are taken over by a longer time scale, some of these features get averaged out, showing the dynamic nature of the spatial image. However, over longer time scales, there is a thermal drift that blurs out some of the contrast in the images of spatial fluctuation. Due to these effects, the time scale associated with the spatial fluctuations cannot be uniquely specified. As a result no tight correlation between the temporal fluctuation and the spatial fluctuation data can be established although we could image the spatial fluctuation.

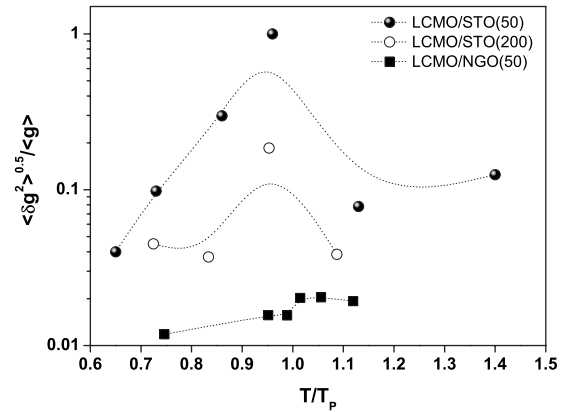


FIG. 10.  $\langle \Delta g^2 \rangle^{0.5} / g$  calculated from line scans across LCMAPs of LCMO/STO (50 nm), LCMO/STO (200 nm), and LCMO/NGO films as a function of temperature.

### V. CONCLUSIONS

We have performed investigation of very low frequency resistance fluctuations in  $\text{La}_{0.67}\text{Ca}_{0.33}\text{MnO}_3$  films. Films with low strain, with uniform strain as well as strain relaxed films were studied. In particular, in films with quenched disorder, there is a significant drop in the noise. The fluctuation arises due to phase coexistence and has a distinct dependence on applied magnetic field. The saturation of total fluctuations in presence of magnetic field was observed. This can be understood by taking into account the strong coupling of magnetic and resistance fluctuations through the mechanism of magnetoresistance. The magnetic fluctuation is found to have a contribution from both domain rotations as well as from coexisting phases. It is observed that the strain and microstructure play an important role in determining the noise power as well as the spectral nature of the resistance fluctuation in manganite films.

### ACKNOWLEDGMENTS

The authors thank the Department of Science and Technology, Government of India for financial support.

\*sudeshna@bose.res.in

†On leave from Indian Institute of Science. arup@bose.res.in

‡joy.mitra@qub.ac.uk

<sup>1</sup> *Colossal Magnetoresistance, Charge Ordering and Related Properties of Manganese Oxides*, edited by C. N. R. Rao and B. Raveau (World Scientific, Singapore, 1998); *Colossal-Magnetoresistive Oxides*, edited by Y. Tokura (Gordon and Breach, New York, 1999).

<sup>2</sup> H. Y. Hwang, S. W. Cheong, N. P. Ong, and B. Batlogg, *Phys. Rev. Lett.* **77**, 2041 (1996); T. V. Ramakrishnan, *J. Phys.: Condens. Matter* **19**, 125211 (2007).

<sup>3</sup> E. Dagotto, T. Hotta, and A. Moreo, *Phys. Rep.* **344**, 1 (2001); *Nanoscale Phase Separation and Colossal Magnetoresistance*, edited by E. Dagotto (Springer-Verlag, Berlin, 2002).

<sup>4</sup> *Electronic Noise and Fluctuations in Solids*, edited by S. Kogan (Cambridge University Press, Cambridge, England, 1996).

<sup>5</sup> H. T. Hardner, M. B. Weissman, M. Jaime, R. E. Treece, P. C. Dorsey, J. S. Horwitz, and D. B. Chrisey, *J. Appl. Phys.* **81**, 272 (1997).

<sup>6</sup> B. Raquet, A. Anane, S. Wirth, P. Xiong, and S. von Molnár, *Phys. Rev. Lett.* **84**, 4485 (2000).

<sup>7</sup> R. D. Merithew, M. B. Weissman, F. M. Hess, P. Spradling, E. R.



- Nowak, J. O'Donnell, J. N. Eckstein, Y. Tokura, and Y. Tomioka, *Phys. Rev. Lett.* **84**, 3442 (2000).
- <sup>8</sup>F. M. Hess, R. D. Merithew, M. B. Weissman, Y. Tokura, and Y. Tomioka, *Phys. Rev. B* **63**, 180408(R) (2001).
- <sup>9</sup>Aveek Bid, Ayan Guha, and A. K. Raychaudhuri, *Phys. Rev. B* **67**, 174415 (2003).
- <sup>10</sup>A. Anane, B. Raquet, S. von Molnar, L. Pinsard-Godard, and A. Revcolevschi, *J. Appl. Phys.* **87**, 5025 (2000).
- <sup>11</sup>Ayan Guha, Arindam Ghosh, and A. K. Raychaudhuri, *Appl. Phys. Lett.* **75**, 3381 (1999).
- <sup>12</sup>C. Barone, C. Adamo, A. Galdi, P. Orgiani, A. Yu. Petrov, O. Quaranta, L. Maritato, and S. Pagano, *Phys. Rev. B* **75**, 174431 (2007).
- <sup>13</sup>Akilan Palanisami, M. B. Weissman, and N. D. Mathur, *Phys. Rev. B* **71**, 014423 (2005).
- <sup>14</sup>Y. Yuzhelevski, V. Dikovskiy, V. Markovich, G. Gorodetsky, G. Jung, D. A. Shulyatev, and Ya. M. Mukovskii, *Fluct. Noise Lett.* **1**, L105 (2001).
- <sup>15</sup>Mandar Paranjape, Ph.D. thesis, Indian Institute of Science, 2003.
- <sup>16</sup>Mandar Paranjape, A. K. Raychaudhuri, N. D. Mathur, and M. G. Blamire, *Phys. Rev. B* **67**, 214415 (2003).
- <sup>17</sup>Barnali Ghosh, Loveleen K. Brar, Himanshu Jain, and A. K. Raychaudhuri, *J. Phys. D* **37**, 1548 (2004).
- <sup>18</sup>Sohini Kar, Jayanta Sarkar, Barnali Ghosh, and A. K. Raychaudhuri, *Phys. Rev. B* **74**, 085412 (2006).
- <sup>19</sup>J. H. Scofield, *Rev. Sci. Instrum.* **58**, 985 (1987).
- <sup>20</sup>A. K. Raychaudhuri, *Curr. Opin. Solid State Mater. Sci.* **6**, 67 (2002).
- <sup>21</sup>P. Reutler, A. Bensaid, F. Herbristrit, C. Höfener, A. Marx, and R. Gross, *Phys. Rev. B* **62**, 11619 (2000).
- <sup>22</sup>F. N. Hooge, *Phys. Lett.* **29A**, 139 (1969); F. N. Hooge, *Physica B & C* **83**, 14 (1976).
- <sup>23</sup>N. D. Mathur and P. B. Littlewood, *Solid State Commun.* **119**, 271 (2001).